PCCP

PAPER

View Article Online
View Journal | View Issue

Cite this: *Phys. Chem. Chem. Phys.*, 2019, **21**, 24935

Selective conformational control by excitation of NH imino vibrational antennas†

Sándor Góbi, *[a] Igor Reva, [a] István Pál Csonka, [b] Cláudio M. Nunes, [a] György Tarczay [bc] and Rui Fausto [ad]

Received 1st October 2019,
Accepted 25th October 2019

DOI: 10.1039/c9cp05370k

rsc.li/pccp

An imino group was used for the first time as a vibrational antenna to manipulate molecular conformations. Imino-thiol isomers of thioacetamide were generated upon UV-irradiation of its amino-thione tautomer isolated in argon matrices at 11 K. Selective and reversible conformational isomerizations were induced by narrowband near-IR irradiation tuned at the frequencies of the 2ν(NH) first stretching overtone of each imino-thiol isomer. The conformational isomerization concerns the change in the orientation of a remote –SH group, while the orientation of the imino (C=NH) group remains the same. Supported by quantum chemical anharmonic computations, this allowed for a reliable, isomer-selective vibrational assignment of the four imino-thiol isomers extending now over the full mid-IR and near-IR ranges. It was found that the experimental IR intensities of the 2ν(NH) first stretching overtones (computed 4–5 km mol^{-1}) of the imino-thiol forms are comparable to those of the ν(NH) stretching fundamentals (computed 2–4 km mol^{-1}). This is the first time such a phenomenon is reported for an imine molecule. The kinetics of conformational isomerization was monitored *in situ*, indicating that the irradiation-induced processes are significantly faster than the tunneling-driven spontaneous *cis–trans* rotamerization of the –SH group. Quantum yields for the rotamerizations of the –SH group resulting from the vibrational excitation of a remote –NH group were estimated and found to be comparable to those observed for matrix-isolated carboxylic acids and amino acids, where conformational changes of the –OH group were induced by the direct vibrational excitation of 2ν(OH) first stretching overtones.

1. Introduction

The infrared (IR) spectroscopy of compounds containing thiocarbonyl groups has a long history.[1,2] In a similar way to their oxygen analogues, which are prone to oxo/hydroxyl tautomerism, these compounds exhibit thione/thiol tautomerism. In general, the thione forms are lower in energy than the thiol forms, so that the compounds predominantly or almost exclusively exist in the thione form. Nevertheless, thiones can be readily converted to their higher-energy thiol isomers upon ultraviolet (UV) irradiation.[3,4] If embedded in an inert solid matrix at low temperature, the photogenerated thiol forms can then be preserved and characterized by conventional steady-state spectroscopic methods.

Compared to the commonly found thione tautomer, the elusive thiol isomeric forms might be considered to represent more attractive systems for investigation, in part because they contain the –SH moiety, whose relevance in biochemistry and astrophysics has been gaining recognition during the last few decades. For example, methanethiol has been reported to exist in the interstellar medium long ago,[5] and other thiols (*e.g.*, ethanethiol)[6,7] have also recently been suggested to be present in outer space; making this type of compounds of great interest for both the astrochemical and laboratory astrophysics communities.[8–14] On the other hand, the thiol group may give rise to conformational isomerism, which may have a great impact on the molecular structure and properties of bioactive molecules (for instance, on the pK values and the hydrogen donor/acceptor ability of cysteine, and thus on enzymes' activity).[15–17] Therefore, unraveling the –SH conformational properties in small model compounds is also of great interest. In this context, investigations on the structure, conformational preferences and spectroscopic properties of isolated molecules containing the –SH fragment, like the imino-thiol (or for short, thiol) isomeric forms of thioacetamide, as well as on their UV- or IR-induced reactivity, are of prime importance.

Thioacetamide (C_2H_5NS) is a prototype compound representative of thiocarbonyl compounds, which has been investigated in

[a] *CQC, Department of Chemistry, University of Coimbra, Rua Larga 3004–535, Coimbra, Portugal. E-mail: sgobi@qui.uc.pt*
[b] *MTA-ELTE Lendület Laboratory Astrochemistry Research Group, Institute of Chemistry, ELTE Eötvös Loránd University, P.O. Box 32, H–1518 Budapest, Hungary*
[c] *Laboratory of Molecular Spectroscopy, Institute of Chemistry, ELTE Eötvös Loránd University, P.O. Box 32, H–1518 Budapest, Hungary*
[d] *Chemistry Department, King Fahd University of Petroleum and Minerals, Dhahran, KSA–31261, Saudi Arabia*

† Electronic supplementary information (ESI) available. See DOI: 10.1039/c9cp05370k

some detail before. In the past, it has been used as an organic solvent in the leather, textile, and paper industries, as an accelerator in the vulcanization of rubber, and as a stabilizer of motor fuel.[18,19] However, since it has been recognized as a potential carcinogenic substance,[20,21] the main applications are limited and it is used as a replacement for hydrogen sulfide in qualitative analyses[22] or as a reactant for metal salt nanoparticle synthesis.[23–28] The first study reporting the mid-IR spectrum of matrix-isolated thioacetamide was published a quarter of a century ago.[29] The authors performed an empirical assignment of the IR spectrum of the compound (for the most stable thione form), including some of its deuterated isotopologues. Furthermore, based on the measured vibrational frequencies, they were able to estimate the internal rotation barrier about the C–N bond, which they discussed in comparison with that previously estimated for acetamide in order to evaluate the effect of oxygen-by-sulfur replacement on this property. Although the thione–thiol tautomerization has been subject of many investigations,[30–41] to the best of our knowledge, the thiol forms of thioacetamide have only been described to some extent by two studies. First, the photogeneration of the thiol tautomeric forms of thioacetamide by broadband UV irradiation of the thione tautomer has been reported by Lapinski *et al.*[3] Secondly, our recent study reported the first experimentally observed conformational isomerization of an –SH fragment taking place by quantum tunneling.[4]

Near-IR irradiation-induced *cis–trans* conformational changes in hydroxyl-containing compounds isolated in inert matrices is an extensively studied topic. Carboxylic acids[42–44] such as formic,[45–49] acetic,[50–52] propionic,[53] and pyruvic,[54] for example, were studied successfully using this approach, alongside some dicarboxylic acids,[55–58] and derivatives containing heteroatoms such as nitrogen (oxamic acid),[59] or halogen atoms (*e.g.*, trifluoroacetic,[60] trichloroacetic,[61] tribromoacetic,[62] and 2-chloropropionic acid).[63] Conformational changes involving –OH groups of cyclic and heterocyclic organic acid compounds have also been investigated using the same experimental approach,[64–68] as well as those occurring in carbonic acid,[69] amino acids,[70–74] and nucleobases or nucleobase derivatives.[75–77] The technique has been recently proved to be also useful to induce conformational changes around a particular bond using a remotely located vibrational antenna, *i.e.*, shown to be capable of efficiently modifying the conformation of a group placed several bonds away from the moiety which is vibrationally excited.[53,58,78–86] Although the conformational changes resulting from near-IR irradiation of hydroxy derivative compounds are well-studied, the same does not apply for their sulfur counterparts. Indeed, to the best of our knowledge, only two studies have been published describing near-IR-induced rotamerizations of the thiol group: (i) –SH torsion in cysteine, coupled with other conformational changes, resulting from vibrational excitation of the –OH group,[73] and (ii) –SH flip in thiocytosine, upon excitation of the $-NH_2$ group.[86] As described in detail below, we show that IR-induced –SH rotamerizations are in fact not just feasible, but they can be efficiently controlled in a very selective way. Imino-thiol forms of thioacetamide were generated by narrowband UV irradiation of the amino-thione form isolated in a low-temperature argon matrix. Then, by applying narrowband near-IR excitation to the first stretching overtone of the imino group (2ν(NH)), a selective interconversion between the thiol forms was achieved (resulting from the controlled internal rotation of the –SH moiety). This allowed us to undertake an unprecedented structural and spectroscopic characterization of these species, strongly improving the data reported previously. Moreover, the present study is the first of its kind describing the use of an imino C═NH group as a vibrational antenna to control molecular conformations.

2. Experimental methods

2.1. MI-IR spectroscopy

The experiments were carried out in two laboratories, in Coimbra (Portugal) and in Budapest (Hungary).

In Coimbra, a commercial sample of thioacetamide obtained from Merck (99%) was used. The sample was placed in a small glass oven, connected to the vacuum chamber of a cryostat *via* a stainless steel gate valve. Before the experiments, the sample was pumped through the vacuum chamber at room temperature in order to eliminate air and other trapped volatile impurities. To increase the vapor pressure and achieve the desired sublimation rate of thioacetamide, the sample was slightly heated during deposition to *ca.* 40 °C. A CsI window was used as an optical substrate and was cooled down using a closed-cycle helium refrigerator with a DE-202 expander (Advanced Research Systems) with a base pressure of approximately 10^{-7} mbar. The temperature of the cold window was measured directly by a silicon diode sensor connected to a LakeShore 331 digital temperature controller, which also enables the stabilization of the sample temperature with an accuracy of 0.1 degrees. The vapors of thioacetamide were codeposited with an excess of Ar (Air Liquide, purity 99.9999%) onto the optical substrate kept at 16 K. The temperature of the matrix was lowered to 11 K after finishing deposition. During and after the deposition of the matrix, mid-IR spectra were collected (128 scans) using a Nicolet 6700 FT-IR spectrometer equipped with a Ge/KBr beamsplitter and a mercury cadmium telluride (MCT) detector cooled with liquid nitrogen. The spectral resolution was 0.5 cm^{-1} for the mid-IR region (4000–400 cm^{-1}). In some experiments, to partially protect the matrices from the broad-band radiation of the spectrometer beam source, spectra were collected in the 870–400 cm^{-1} region, using a Spectrogon LP11500 longwave-pass cut-off filter (transmitting only below 870 cm^{-1}) placed between the spectrometer light source and the cryostat.

In Budapest, a commercial sample of thioacetamide obtained from Sigma-Aldrich (>99.0%) was used. The compound was kept in a glass tube with a Young valve, connected to the vacuum chamber of a cryostat, and, before the experiments, the sample was pumped through the vacuum chamber in order to eliminate air and other trapped volatile impurities. The CsI optical substrate of the cryostat was cooled down to 15 K using a closed-cycle helium refrigeration system (Janis CCS-350R cold head cooled by a CTI Cryogenics 22 refrigerator) with a base pressure of

approximately 10^{-6} mbar. The temperature of the cold window was measured by a silicon diode sensor connected to a LakeShore 321 digital temperature controller. The sample vapor was co-deposited with an excess of Ar (Messer, 99.9999%) onto the substrate. The sample sublimation temperature was 318 ± 5 K. The temperature of the matrix was lowered to 11 K after deposition. The mid-IR spectra obtained during and after the deposition of the samples were collected (64 scans) in the 4000–400 cm^{-1} region with a 1 cm^{-1} resolution using a Bruker IFS 55 FT-IR spectrometer equipped with a KBr beamsplitter and an MCT detector cooled with liquid nitrogen.

2.2. Irradiation experiments

In Coimbra, the matrices were irradiated after deposition, through the outer KBr window of the cryostat. For this, we used frequency-tunable narrowband light provided by an Optical Parametric Oscillator (OPO, Spectra-Physics MOPO-SL, FWHM ≈ 0.2 cm^{-1}, pulse duration = 10 ns) pumped with a pulsed Nd:YAG laser (Spectra-Physics PRO-230, output power (P) ≈ 4.5 W, wavelength (λ) = 355 nm, repetition rate (f) = 10 Hz). The OPO was equipped with a frequency-doubling unit (Spectra-Physics MOPO FDO-970). For the UV and near-IR irradiation, the frequency-doubled signal beam (P ≈ 9 mW) and the idler beam (P ≈ 5–30 mW) of the OPO were used, respectively.

The deposited matrix in the Budapest experiment was irradiated *in situ* through the outer quartz window of the cryostat applying a tunable narrowband signal beam provided by an OPO (GWU/Spectra-Physics VersaScan MB 240, FWHM ≈ 5 cm^{-1}) pumped by a pulsed Nd:YAG laser (Spectra-Physics Quanta Ray Lab 150, P ≈ 2.1–2.2 W, λ = 355 nm, f = 10 Hz, pulse duration = 2–3 ns). The OPO was equipped with a frequency-doubling unit (Spectra-Physics uvScan). The CsI cold window was tilted at 45° with respect to the beam path of the FT-IR spectrometer, whereas the OPO beam was perpendicular to the FT-IR beam, allowing for simultaneous irradiation and spectral collection. The value of P of the frequency-doubled signal beam used for the UV and the idler beam for the near-IR irradiation was 25 mW and 130–135 mW, respectively. In order to allow for the collection of FT-IR spectra during near-IR irradiation, an LPW 3860 low-pass-filter was placed between the detector of the spectrometer and the cold window.

2.3. Theoretical computations

The quantum chemical computations were performed by using Becke's three parameter hybrid functional B3LYP, with the non-local and local correlation described by the Lee–Yang–Parr and the Vosko–Wilk–Nusair III functionals, respectively,[87–89] with Pople's 6-311++G(3df,3pd) basis set[90] as implemented in Gaussian 09.[91] The initial geometry optimizations were followed by anharmonic vibrational frequency computations. A fully automated second-order vibrational perturbative approach (VPT2) of Barone and coworkers was applied in these calculations.[92,93] This approach allows the evaluation of anharmonic vibrational wavenumbers and anharmonic IR intensities up to two quanta, including fundamental transitions, first overtones and combination transitions.[93–95] The computed anharmonic vibrational wavenumbers were not scaled. For a graphical comparison of the theoretical spectra with the experimental ones, the simulated mid-IR spectra were obtained using the theoretical anharmonic vibrational frequencies and computed IR intensities by convoluting them with Lorentzian functions with an FWHM of 0.5 cm^{-1} in the Synspec software.[96] Note that the peak intensities in the simulated spectra (shown in units of "relative intensity" in the ESI†) differ from the calculated IR intensities (in km mol^{-1}), because Synspec produces an output which satisfies the condition that the integrated band area in the simulated spectrum is equal to the calculated IR intensity.

The energies of isomerization barriers were obtained by optimizing the minima and transition states at the B2PLYP/6-311++G(3df,3pd) level of theory using the Berny algorithm.[97,98] The optimizations of the stationary points were followed by vibrational computations at the same level, in order to account for zero-point vibrational energy corrections.

3. Results and discussion

3.1. UV-generation of thiol isomeric forms of thioacetamide from the thione form

As it has been previously reported, only the amino-thione (**Tn**) form of thioacetamide can be observed after matrix deposition.[3,4] The UV absorption of thioacetamide is characterized by an onset near 300 nm and a maximum near 266 nm.[99] With this information in mind, freshly-deposited matrices of thioacetamide were irradiated using UV light with λ = 265 nm for 6 min (in Coimbra), or λ = 275 nm for 60 min (in Budapest). Upon irradiation, **Tn** was consumed giving rise to the imino-thiol forms.[3] They have two conformational degrees of freedom, defined by the HN═CS and NC–SH dihedral angles, both of which adopt values equal to 0° or 180° in the minimum energy structures. The minimum energy orientations around the double N═C bond are designated in this study as *syn* (**s**) and *anti* (**a**), while those around the single C–S bond are denoted as *cis* (**C**) and *trans* (**T**). The four possible thiol structures are therefore named **aC**, **aT**, **sC**, and **sT** (Scheme 1). Fig. S1–S8 (ESI†) show the changes in the IR spectra resulting from the UV irradiation experiments (at λ = 265 nm), together with the simulated spectra of all thioacetamide forms (thione and the four thiol isomers). Both the mid-IR and near-IR spectral regions were monitored before and after UV irradiation, thus allowing us to clearly identify the set of initially existing bands (due to the **Tn** form, Table 1). Furthermore, the new absorptions due to the UV-generated thioacetamide thiol forms in the whole spectral range from 400 cm^{-1} up to 7200 cm^{-1} were observed as well. This permitted us to considerably extend the spectroscopic information on the studied compound reported to date.[3,4]

3.2. Selective SH rotamerization induced by near-IR irradiation

It has been noticed earlier that the thiol forms of thioacetamide undergo conformational isomerization when exposed to the broadband-light globar source of an FT-IR spectrometer.[4] In the present work, attempts were made to identify the vibrational

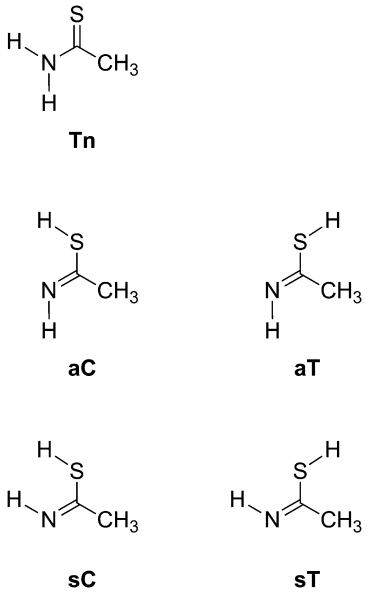

Scheme 1 Structures of the amino-thione (**Tn**) and four imino-thiol (**aC**, **aT**, **sC**, and **sT**) forms of thioacetamide.

transitions that may be responsible for such transformations, as described below.

As mentioned in the Introduction, molecules containing –OH groups may undergo conformational isomerization upon excitation of their first stretching overtones 2ν(OH). Moreover, it has been found before that vibrational excitation of the first stretching overtone of the aromatic NH group in indole derivatives induces conformational changes, including rearrangements implying rotation of other groups in the molecule.[80,81] By analogy, one could expect that the excitation of the first stretching overtones of the thiol (2ν(SH)) and/or imino C═NH (2ν(NH)) group might result in conformational changes in the thiol isomers of thioacetamide. However, the 2ν(SH) first stretching overtone can be anticipated to be of very low intensity (the average computed IR intensity for the thioacetamide thiol isomers is $\approx$0.3 km mol^{-1}) and bands due to the different isomers are expected to be quite close in frequency (calculated range 5022–5008 cm^{-1}; *i.e.*, $\Delta\nu \approx$ 14 cm^{-1}). In addition, the spectral range in which they appear is not accessible to our laser/MOPO system (the available minimum frequency $\approx$6000 cm^{-1}), therefore the use of this mode to perform the IR-excitation experiments could not be attempted. Hence, the next task of this work consisted in the identification of the spectral signatures of the thiol forms in the range where bands due to the 2ν(NH) first stretching overtone are expected. It should be noted that the bands of the ν(NH) stretching fundamental were also predicted by the calculations as being of low intensity (ranging between 1.8 and 4.1 km mol^{-1}; Tables 2–5). These bands were assigned for the first time in the present study (Fig. 1). Noticeably, the anharmonic frequency computations predict the IR intensities of the 2ν(NH) first stretching overtone modes to be equal to or even higher than those corresponding to the ν(NH) stretching fundamental modes (Tables 2–5). This interesting phenomenon has been reported by Kjaergaard *et al.* for primary and secondary amines,[100–102] however, to the best of our knowledge, no molecules with imino groups have been reported exhibiting the same peculiarity so far.

Table 1 IR spectrum of the **Tn** amino-thione tautomer of thioacetamide

Wavenumber (cm^{-1})					
Experim.[a]	Theor.[b]	$I_{exp.}$[c]	$I_{theor.}$[b]	Symm.	Assignment[d]
6985	6983	0.8	2.3	A′	$2\nu_{as}(NH_2)$
6790	6805	1.7	2.1	A′	$\nu_{as}(NH_2) + \nu_s(NH_2)$
6721	6757	2.5	2.2	A′	$2\nu_s(NH_2)$
5095	5109	2.2	2.0	A′	$\nu_{as}(NH_2) + \beta(NH_2)$
4994	5008	0.3	0.4	A′	$\nu_s(NH_2) + \beta(NH_2)$
4860	4873	0.2	0.2	A′	$\nu_{as}(NH_2) + \nu$(C–N)
4827	4835	1.6	2.5	A′	$\nu_{as}(NH_2) + \rho(NH_2)$
4711	4719	0.4	0.6	A′	$\nu_s(NH_2) + \rho(NH_2)$
4507	4496	0.5	1.1	A′	$\nu_{as}(NH_2) + \nu$(C–C)
4109	4133	0.4	0.4	A″	$\nu_{as}(NH_2) + \tau(NH_2)$
3521	3531	67	25	A′	$\nu_{as}(NH_2)$
3413sh, 3405	3414	59	21	A′	$\nu_s(NH_2)$
3176	3178	2.1	1.8	A′	$2\beta(NH_2)$
3030	3055	0.6	8.0	A′	$\nu_{as}(CH_3) + \tau(CH_3)$
2964	3017	3.3	2.2	A′	$\nu_{as}(CH_3)$
2941	2932	0.9	6.3	A″	$\nu_{as}(CH_3)$
2925	2916	7.2	19	A′	$\nu_s(CH_3)$
2902	2901	0.4	0.5	A′	$\beta(NH_2) + \rho(NH_2)$
2725	2727	0.5	0.6	A′	$2\beta_s(CH_3)$
2685	2679	0.2	0.4	A′	2ν(C–N)
2677	2677	0.2	0.1	A′	$\beta_s(CH_3) + \rho(NH_2)$
2655	2649	0.8	0.8	A′	ν(C═N) + $\rho(NH_2)$
2592	2596	0.3	0.2	A″	$\beta(NH_2) + \rho(CH_3)$
2544	2561	0.5	1.2	A′	$\beta(NH_2) + \nu$(C–C)
2072	2077	0.7	0.8	A′	ν(C–N) + ν(C═S)
1978	1938	0.7	1.2	A′	2ν(C–C)
	1933		1.1	A″	$\beta(NH_2) + \omega(NH_2)$
1597	1599	140	121	A′	$\beta(NH_2)$
1457	1437	4.4	4.1	A″	$\beta_{as}(CH_3)$
1441	1433	7.8	12	A′	$\beta_{as}(CH_3)$
1380	1380	18	15	A′	$\rho(CH_3) + \beta$(CCS)
1369	1372	49	21	A′	$\beta_s(CH_3)$
1346	1348	183	222	A′	ν(C–N)
1312	1309	21	33	A′	$\rho(NH_2)$
1168	1189	1.4	2.8	A′	$2\tau(NH_2)$
1018	1003	3.2	7.7	A′	2γ(CS)
999	999	14	8.3	A′	$\rho(CH_3)$
997	987	10	42	A′	ν(C–C)
944, 939sh, 938	895	19	8.9	A′	$\omega(NH_2) + \tau(NH_2)$
780sh, 776sh, 774	733	56	85	A′	$2\omega(NH_2)$
729	735	13	2.2	A′	ν(CS)
592	603	7.6	13	A″	$\tau(NH_2)$
508	501	7.4	13	A″	γ(CS)
426	434	1.6	1.8	A′	β(NCS)

[a] Isolated in an Ar matrix at 11 K. sh: shoulder. [b] Anharmonic wavenumbers (unscaled) and anharmonic infrared intensities (km mol^{-1}) computed at the B3LYP/6-311++G(3df,3pd) level of theory. [c] Normalized experimental band areas. The values were obtained by multiplying the integrated area of a band in the experimental infrared spectrum by the sum of the theoretical infrared intensities then dividing by the sum of the experimental band areas. [d] ν: stretching, β: in-plane bending, γ: out-of-plane bending, ρ: rocking, ω: wagging, τ: torsional, s: symmetric, as: antisymmetric vibrations.

The full 2ν(NH) spectral range is shown in Fig. S1 (ESI†). The **Tn** form gives rise to three well-identified absorptions between 7000 and 6700 cm^{-1} (at 6985, 6790, and 6721 cm^{-1}; see Table 1 for assignments). The new bands appearing upon UV-irradiation are found at much lower wavenumbers, around 6400 cm^{-1} (see Fig. 1b for an expansion of this spectral range). The obtained agreement between the observed bands (6422, 6405, 6398, and 6378 cm^{-1}) and the anharmonic computed wavenumbers for the

Table 2 IR spectrum of the **aC** imino-thiol tautomer of thioacetamide

Wavenumber (cm^{-1})					
Experim.[a]	Theor.[b]	$I_{exp.}$[c]	$I_{theor.}$[b]	Symm.	Assignment[d]
6378	6384	0.7	5.0	A′	2ν(NH)
4543	4546–4525	N/A	N/A	N/A	N/A[e]
3268	3276	1.9	1.8	A′	ν(NH)
2995[e]	2978	N/A	12	A′	$\nu_{as}(CH_3)$[e]
2984[e]	2956	N/A	5.2	A″	$\nu_{as}(CH_3)$[e]
2981[e]	2935	N/A	6.8	A′	$\nu_{s}(CH_3)$[e]
2979[e]		N/A			
2607	2563	5.2	0.4	A′	ν(SH)
2416	2404	0.3	0.2	A″	$\rho(CH_3) + \beta_s(CH_3)$
1620sh	1640	65	134	A′	ν(C═N)
1440	1439	26	19	A′	$\beta_{as}(CH_3)$
1434, 1430	1429	36	8.6	A″	$\beta_{as}(CH_3)$[f]
1371	1372	31	12	A′	$\beta_{s}(CH_3)$
1313	N/A	N/A	N/A	N/A	N/A
1272	1253	41	55	A′	β(NH)
1050	1041	77	33	A′	$\rho(CH_3)$
1036	1037	15	5.0	A″	$\rho(CH_3)$
991	969	38	53	A′	ν(C–C)?
968	969	20	53	A′	ν(C–C)
849	827	N/A	15	A′	β(SH)
816	807	83	52	A″	τ(NH)
645, 635	621	30	50	A′	ν(C–S)
446	446	11	5.1	A′	β(NCS)

[a] Isolated in an Ar matrix at 11 K. sh: shoulder. [b] Anharmonic wavenumbers (unscaled) and anharmonic infrared intensities (km mol^{-1}) computed at the B3LYP/6-311++G(3df,3pd) level of theory. N/A: unknown. [c] Normalized experimental band areas. The values were obtained by multiplying the integrated area of a band in the experimental infrared spectrum by the sum of the theoretical infrared intensities then dividing by the sum of the experimental band areas. [d] ν: stretching, β: in-plane bending, ρ: rocking, τ: torsional, s: symmetric, as: antisymmetric vibrations, ?: tentative assignment. [e] Unequivocal assignment could not be done due to extensive overlap. [f] Contribution of *syn*-forms cannot be excluded.

Table 3 IR spectrum of the **aT** imino-thiol tautomer of thioacetamide

Wavenumber (cm^{-1})					
Experim.[a]	Theor.[b]	$I_{exp.}$[c]	$I_{theor.}$[b]	Symm.	Assignment[d]
6405	6417	0.5	4.6	A′	2ν(NH)
4543	4546–4525	N/A	N/A	N/A	N/A[e]
3282	3291	1.0	2.1	A′	ν(NH)
3002[e]	2971	N/A	15	A′	$\nu_{as}(CH_3)$[e]
2987[e]	2956	N/A	6.0	A″	$\nu_{as}(CH_3)$[e]
2976[e]	2933	N/A	8.4	A′	$\nu_{s}(CH_3)$[e]
2614	2564	0.7	2.1	A′	ν(SH)
1621	1642	145	139	A′	ν(C═N)
1441	1440	20	15	A′	$\beta_{as}(CH_3)$
1433	1433	29	9.0	A″	$\beta_{as}(CH_3)$[f]
1368sh	1370	32	11	A′	$\beta_{s}(CH_3)$
1318	N/A	N/A	N/A	N/A	N/A
1281	1254	42	64	A′	β(NH)
1270	1244	10	2.5	A′	2ν(NH)
1072sh	N/A	N/A	N/A	N/A	N/A
1047	1037	68	55	A′	$\rho(CH_3)$
1037	1040	12	3.8	A″	$\rho(CH_3)$
1000sh	981	19	51	A′	ν(C–C)?
978	981	16	51	A′	ν(C–C)
891, 890	872	9.0	13	A′	β(SH)
818	812	65	53	A″	τ(NH)
640	624	36	49	A′	ν(C–S)
431	430	2.2	1.7	A′	β(NCS)

[a] Isolated in an Ar matrix at 11 K. sh: shoulder. [b] Anharmonic wavenumbers (unscaled) and anharmonic infrared intensities (km mol^{-1}) computed at the B3LYP/6-311++G(3df,3pd) level of theory. N/A: unknown. [c] Normalized experimental band areas. The values were obtained by multiplying the integrated area of a band in the experimental infrared spectrum by the sum of the theoretical infrared intensities then dividing by the sum of the experimental band areas. [d] ν: stretching, β: in-plane bending, ρ: rocking, ω: wagging, τ: torsional, s: symmetric, as: antisymmetric vibrations, ?: tentative assignment. [e] Unequivocal assignment could not be done due to extensive overlap. [f] Contribution of *syn*-forms cannot be excluded.

Table 4 IR spectrum of the **sC** imino-thiol tautomer of thioacetamide

Wavenumber (cm^{-1})					
Experim.[a]	Theor.[b]	$I_{exp.}$[c]	$I_{theor.}$[b]	Symm.	Assignment[d]
6422	6434	0.3	4.0	A′	2ν(NH)
4543	4546–4525	N/A	N/A	N/A	N/A[e]
3292	3300	1.7	3.1	A′	ν(NH)
3248	3285	0.8	1.9	A′	2ν(C═N)
3021	3001	1.6	6.0	A′	$\nu_{as}(CH_3)$
2883[e]	2954	N/A	6.6	A″	$\nu_{as}(CH_3)$[e]
2866[e]	2935	N/A	6.3	A′	$\nu_{s}(CH_3)$[e]
2603	2557	3.1	1.3	A′	ν(SH)
2476	2435	0.6	0.8	A′	2β(NH)
1632	1648	130	122	A′	ν(C═N)
1370sh	1371	56	6.0	A′	$\beta_{s}(CH_3)$
1254	1227	107	211	A′	β(NH)
1236	1208	74	17	A′	2ν(C–S)
1070	1058	4.8	24	A′	$\rho(CH_3)$
1051sh	N/A	N/A	N/A	N/A	N/A
1042sh	1042	2.8	3.0	A″	$\rho(CH_3)$
860	851	10	13	A′	β(SH)
836	836	64	53	A″	τ(NH)
623	607	32	37	A′	ν(C–S)
443	437	11	12	A′	β(NCS)

[a] Isolated in an Ar matrix at 11 K. sh: shoulder. [b] Anharmonic wavenumbers (unscaled) and anharmonic infrared intensities (km mol^{-1}) computed at the B3LYP/6-311++G(3df,3pd) level of theory. N/A: unknown. [c] Normalized experimental band areas. The values were obtained by multiplying the integrated area of a band in the experimental infrared spectrum by the sum of the theoretical infrared intensities then dividing by the sum of the experimental band areas. [d] ν: stretching, β: in-plane bending, ρ: rocking, τ: torsional, s: symmetric, as: antisymmetric vibrations. [e] Unequivocal assignment could not be done due to extensive overlap.

Table 5 IR spectrum of the **sT** imino-thiol tautomer of thioacetamide

Wavenumber (cm^{-1})					
Experim.[a]	Theor.[b]	$I_{exp.}$[c]	$I_{theor.}$[b]	Symm.	Assignment[d]
6398	6413	0.3	4.0	A′	2ν(NH)
4543	4546–4525	N/A	N/A	N/A	N/A[e]
3276	3289	2.4	4.1	A′	ν(NH)
3015	2996	3.1	8.4	A′	$\nu_{as}(CH_3)$
2933[e]	2954	N/A	7.9	A″	$\nu_{as}(CH_3)$[e]
2891[e]	2937	N/A	7.7	A′	$\nu_{s}(CH_3)$[e]
2609	2558	0.7	1.4	A′	ν(SH)
1627	1645	168	74	A′	ν(C═N)
1368	1370	51	11	A′	$\beta_{s}(CH_3)$
1267	1243	244	212	A′	β(NH)
1244	1210	54	14	A′	2ν(C–S)
1063	1054	29	22	A′	$\rho(CH_3)$
1043, 1041	1042	8.3	2.3	A″	$\rho(CH_3)$
869	857	8.0	7.1	A′	β(SH)
849	849	108	50	A″	τ(NH)
626	608	43	35	A′	ν(C–S)
421	416	5.4	13	A′	β(NCS)

[a] Isolated in an Ar matrix at 11 K. sh: shoulder. [b] Anharmonic wavenumbers (unscaled) and anharmonic infrared intensities (km mol^{-1}) computed at the B3LYP/6-311++G(3df,3pd) level of theory. N/A: unknown. [c] Normalized experimental band areas. The values were obtained by multiplying the integrated area of a band in the experimental infrared spectrum by the sum of the theoretical infrared intensities then dividing by the sum of the experimental band areas. [d] ν: stretching, β: in-plane bending, ρ: rocking, τ: torsional, s: symmetric, as: antisymmetric vibrations. [e] Unequivocal assignment could not be done due to extensive overlap.

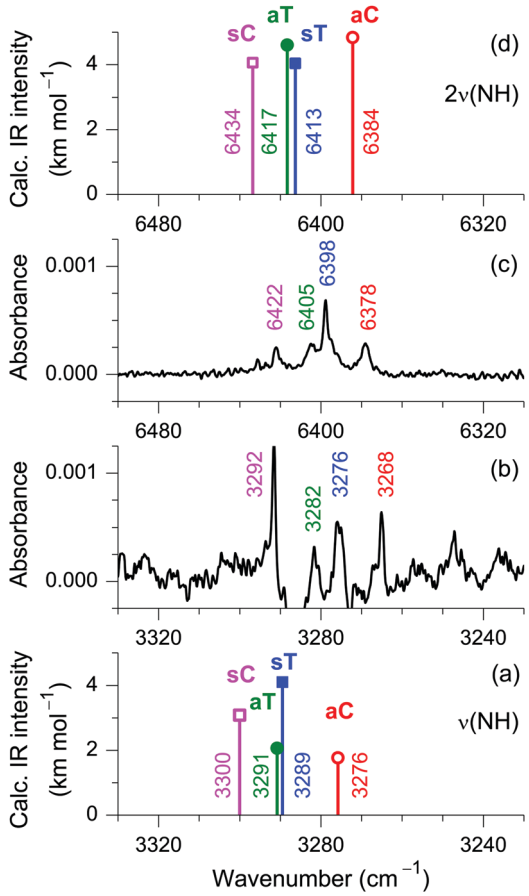

Fig. 1 Fragments of the mid-IR (b) and near-IR (c) difference spectra, showing the new bands of photoproducts growing upon UV irradiation of thioacetamide isolated in an argon matrix at 11 K. The experimental bands are compared with the anharmonic wavenumbers (unscaled) and IR intensities of the ν(NH) (a) and 2ν(NH) (d) vibrations of the **sC** (pink, open square), **sT** (blue, closed square), **aT** (green, closed circle), and **aC** (red, open circle) imino-thiol forms calculated at the B3LYP/6-311++G(3df,3pd) level of theory. Note that the ordinate (intensity) scales of the experimental spectra (b and c) are identical, as well as those of the computed spectra (a and d).

four isomeric thiol forms of thioacetamide (6434, 6417, 6413, and 6384 cm^{-1}, respectively; see Fig. 1d and also Tables 2–5) is remarkable, and allowed for the secure assignment of the bands to the individual **sC**, **aT**, **sT**, and **aC** forms, respectively. Below, we provide further support to this assignment by performing irradiation at the observed 2ν(NH) wavenumbers and by following the induced spectral changes in the full mid-IR range.

3.2.1. 900–800 cm^{-1} spectral region. When exposing the thiol isomeric forms of thioacetamide to near-IR photons with a wavenumber corresponding to the vibrational frequencies of each of the four bands in the 2ν(NH) first stretching overtone region, structural changes were found to be induced in the isolated molecules. These are accompanied by changes in the vibrational spectrum of the matrix previously subjected to UV irradiation in order to generate the thiol forms. One of the most informative spectral regions of the imino-thiol forms is the 860–810 cm^{-1} range, corresponding to the τ(NH) torsional vibrational mode of the imino group (Fig. 2). This is due to the lack of absorption bands of the **Tn** precursor in this region and also because the bands of the four thiol forms can be reliably distinguished, unlike in some other regions where their bands overlap, either with each other or with bands of the precursor. Here, four strong IR bands can be observed due to the τ(NH) torsional mode (849, 836, 818, and 816 cm^{-1}, Fig. 2a).[4] The corresponding computed bands, with IR-intensities near 50 km mol^{-1}, can be found at 849, 836, 812, and 807 cm^{-1} due to **sT**, **sC**, **aT** and **aC**, respectively (Fig. 2d). Upon irradiation at 6422 cm^{-1} (P = 5–30 mW, the exposure time was 15–20 minutes in all cases) the **sC** band at 836 cm^{-1} decreases over time with the simultaneous growth of the **sT** band at 849 cm^{-1} (Fig. 2b). The opposite process can be observed (*i.e.*, **sT** → **sC**: an increasing band at 836 cm^{-1} and a decreasing one at 849 cm^{-1}) when using 6398 cm^{-1} to irradiate the sample (Fig. 2b). If the irradiation is performed at 6405 cm^{-1}, the 818 cm^{-1} band of **aT** decreases simultaneously with the increase of the **aC** band observed at 816 cm^{-1} (Fig. 2c). Finally, the opposite phenomenon can be described (*i.e.*, **aC** → **aT**: an increasing band at 818 cm^{-1} and a decreasing one at 816 cm^{-1}) when irradiation at 6378 cm^{-1} is applied (Fig. 2c). The presented data allowed a detailed identification of four pairs of bands: near-IR bands due to the 2ν(NH) first stretching overtone and the mid-IR bands of the same imino-thiol forms due to the τ(NH) torsional mode. Overall, the different near-IR irradiation induces structural changes in a very selective way, and these changes are limited exclusively to the *syn*- or exclusively to the *anti*-type of isomers (Fig. 3), *i.e.*, they correspond to conformational isomerizations about the single C–S bond. It should be noticed here that the non-observation of isomerization of the imine group is in line with earlier attempts, *i.e.*, this type of isomerization induced by vibrational excitation (using broadband IR radiation) was not detected.[76] In the present case, this result could be anticipated, since the predicted barrier for imine isomerization in thioacetamide with respect to inversion of the C=N double bond is more than 93 kJ mol^{-1} (7800 cm^{-1}, Fig. 4),[4] *i.e.*, considerably higher than the energy of the vibrationally excited modes (about 77 kJ mol^{-1}). It should be noted that excitation of 77 kJ mol^{-1} is significantly higher in energy than the barrier for rotation around the C–S bond (17.1 and 29.5 kJ mol^{-1} or 1430 and 2470 cm^{-1}, Fig. 4).

The findings described above can be generalized to changes observed in the whole spectrum upon narrowband near-IR irradiation. These changes allow classification of the spectral bands into four groups, which define the behavior of the four individual thiol isomers of thioacetamide (Fig. 3 and Table 6): (i) the bands belonging to the first group do not change when the sample is exposed to photons with wavenumbers of 6422 or 6398 cm^{-1}; they decrease when the sample is irradiated at 6378 cm^{-1} and increase when it is irradiated at 6405 cm^{-1}. (ii) The second group of bands also remains the same upon irradiation of the sample at 6422 or 6398 cm^{-1}, but the response is the opposite to that of the first group, *i.e.*, they increase upon irradiation at 6378 cm^{-1} and decrease upon irradiation at 6405 cm^{-1}. (iii) In contrast, the bands of the third group are not altered by the irradiation performed at 6405 or 6378 cm^{-1}, but decrease upon irradiation at 6422 cm^{-1} and

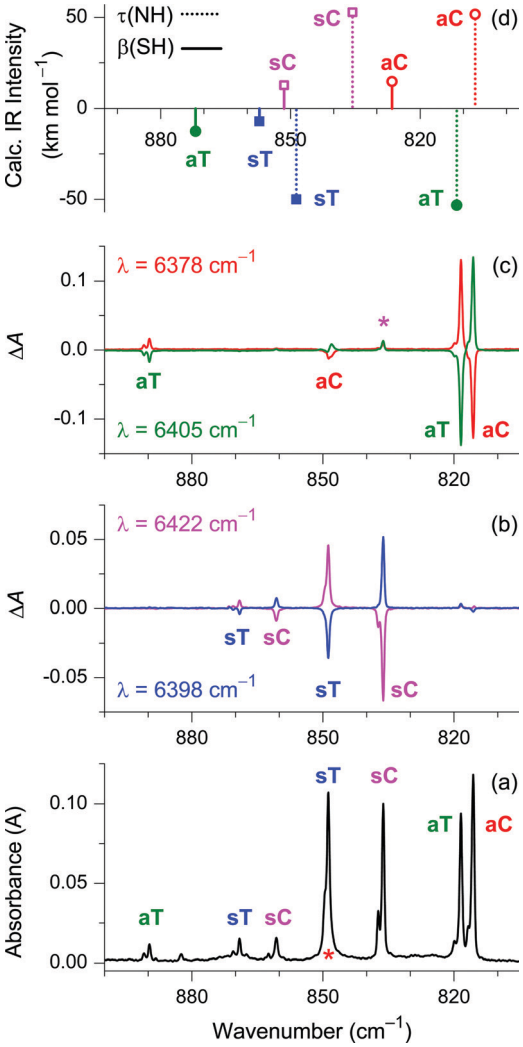

Fig. 2 (a) Experimental mid-IR spectrum, showing the new bands of imino-thiol photoproducts growing upon UV irradiation of thioacetamide isolated in an argon matrix at 11 K; experimental difference spectra showing changes in absorption (ΔA) upon subsequent irradiation of the sample with near-IR light (b) at 6398 cm^{-1} (blue) or at 6422 cm^{-1} (pink); and (c) at 6405 cm^{-1} (green) or at 6378 cm^{-1} (red); (d) anharmonic wavenumbers (unscaled) and IR intensities due to β(SH) (solid line) and τ(NH) (dashed line) modes of **sC** (pink, open squares) and **sT** (blue, closed squares), and **aT** (green, closed circles) and **aC** (red, open circles) imino-thiol forms computed at the B3LYP/6-311++G(3df,3pd) level of theory. The intensities of the **sT** and **aT** forms are multiplied by (−1). The red asterisk in frame (a) designates the position of the weak β(SH) mode due to **aC** overlapped by the strong τ(NH) mode of **sT**. The band in frame (c) designated by an asterisk is due to residual conformational change of the *syn*-form **sC** induced by the unfiltered light of the spectrometer source.

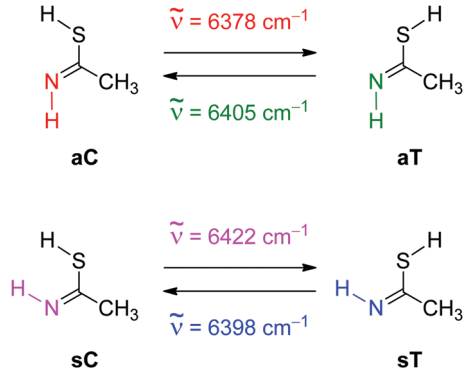

Fig. 3 Selective conformational isomerizations observed for the four imine-thiol isomers of thioacetamide isolated in argon matrices at 11 K. The reactions were induced by monochromatic excitation at the wavenumbers of the corresponding 2ν(NH) vibrational modes.

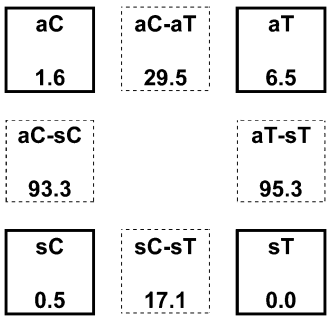

Fig. 4 Zero-point corrected relative energies (in kJ mol^{-1}) of all imino-thiol isomers of thioacetamide (in bold solid rectangles) as well as the relative energies of the first-order transition states (in thin dashed rectangles) separating the minima. All values, with respect to the **sT** form, correspond to geometries optimized at the B2PLYP/6-311++G(3df,3pd) level of theory, and include the zero-point vibrational energy corrections, computed at the same level.

Table 6 Classification of the imino-thiol forms of thioacetamide into four groups depending on their behavior upon narrowband near-IR irradiation[a,b]

Isomer	aC	aT	sC	sT
Wavenumber (cm^{-1})	Set 1	Set 2	Set 3	Set 4
6422	0	0	−	+
6405	+	−	0	0
6398	0	0	+	−
6378	−	+	0	0

[a] The wavenumbers correspond to the new peaks appearing in the near-IR spectrum upon UV-irradiation of the monomeric thioacetamide isolated in an argon matrix at 11 K (see Fig. 2a). [b] Symbols " +", "−", and "0" stand for an increase of the signal, a decrease of the signal, and no change upon irradiation at the given wavenumber, respectively.

increase upon irradiation at 6398 cm^{-1}. (iv) Finally, the fourth group of bands, similarly to the third group, is not affected by the irradiation at 6405 and 6378 cm^{-1}, but upon irradiating at 6422 and 6398 cm^{-1} they increase and decrease, respectively (*i.e.*, behave in the opposite way to the third group). Each one of the four different sets of bands fits closely the computed spectrum of one of the four thioacetamide thiol isomers **aC**, **aT**, **sC** and **sT**, as it can be seen in the data shown in Tables 2–5 (which also provide the band assignments), and in Fig. S9–S16 and Table S1 (ESI†). Such a fact allows doubtless assignment of the four sets of bands to each particular isomer. Below, some representative spectral regions are discussed in more detail. The order in which they are discussed reflects their importance and the novelties that could be extracted from them.

Besides the τ(NH) torsional modes, the bands due to the β(SH) bending modes are expected to appear in this spectral range.[36]

Indeed, the computed for the four thiol forms of thioacetamide (**aT**, **sT**, **sC** and **aC**) predict the β(SH) modes to appear at 872, 857, 851 and 827 cm^{-1}, respectively, all of them with weak absolute IR intensities (15 km mol^{-1} or less, Fig. 2d). The bands belonging to the **aT**, **sT** and **sC** isomers are clearly visible in the experimental spectrum at 890 cm^{-1} (decreases when irradiating at 6405 and increases at 6378 cm^{-1}), 869 cm^{-1} (decreases upon irradiation at 6398 and increases at 6422 cm^{-1}), and 860 cm^{-1} (decreases during irradiation at 6422 and increases at 6398 cm^{-1}), respectively. However, the band of the fourth isomer (**aC**) is not obvious at first glance, and the results from the performed selective near-IR irradiation were needed in order to unambiguously assign it. When irradiating the sample at 6378 and 6405 cm^{-1}, the τ(NH) torsion band belonging to the **sT** isomer is not expected to change, however, a small decrease was observed in the former case and a small increase could be detected in the latter one (Fig. 2c and d). These results allow us to conclude that a weak band due to **aC** (due to its β(SH) bending mode) is superposed by the much more intense τ(NH) torsion band of **sT**.

3.2.2. 660–600 cm^{-1} region. Only one fundamental mode, the ν(C–S) stretching, of each conformer is predicted to be present in this spectral region (Fig. 5). In the case of three isomers (**sT**, **sC**, and **aT**) the experimental spectra match well with the computations (626, 623, and 640 cm^{-1} *vs.* 608, 607, and 624 cm^{-1}, respectively). The band at 626 cm^{-1} decreases when irradiating at 6398 cm^{-1} and increases at 6422 cm^{-1}, whereas the one at 623 cm^{-1} decreases upon irradiation at 6422 cm^{-1} and increases at 6398 cm^{-1} and the one at 640 cm^{-1} decreases when irradiating at 6405 cm^{-1} and increases upon irradiation at 6378 cm^{-1}, respectively. The reason why the experimental absorption band of **aC** appears as a broad split band, with maxima at 645 and 635 cm^{-1} (which decrease and increase upon irradiation at 6378 and 6405 cm^{-1}, respectively, as expected for **aC** bands), is possibly matrix-site splitting. Alternatively, a Fermi-resonance between the fundamental of the ν(C–S) stretching (computed to be at 621 cm^{-1}) and the first overtone of the β(CCS) bending mode (computed value 648 cm^{-1}) of the **aC** isomer could also result in the observed splitting. Moreover, the anharmonic combination of $\tau(CH_3)$ torsion and γ(C–S) out-of-plane bending computed at 603 cm^{-1} may also interact with the ν(C–S) stretching mode, resulting in a Fermi-resonance splitting.

3.2.3. 3320–3260 cm^{-1} region. The experimental bands corresponding to the ν(NH) stretching vibrations of all four imino-thiol forms are very weak (Fig. 6), with peak intensities on the order of 0.001 absorbance units in the collected spectra. Despite the difficulties caused by the low intensity of the bands, their assignment was made possible due to the selective and reversible changes induced by the performed near-IR irradiation as well as due to the good signal-to-noise ratio. According to these experiments, the band at 3292 cm^{-1} is ascribable to the **sC** isomer (computed value: 3300 cm^{-1}) since it decreases upon irradiation at 6422 cm^{-1} and increases upon irradiation at 6398 cm^{-1}. The bands due to the other three isomers (**aT**, **sT** and **aC**) can also be assigned based on their response to the selective near-IR irradiation and are found at 3282, 3276, and 3268 cm^{-1} (theoretical values: 3291, 3289, and 3276 cm^{-1}), respectively. According to the expected patterns of response to near-IR irradiation, the **aT** band at 3282 cm^{-1} decreases and increases upon irradiation at 6405 cm^{-1} and 6378 cm^{-1}, respectively. The **sT** band at 3276 cm^{-1} decreases when the sample is exposed to irradiation at 6398 cm^{-1} and increases upon irradiation at 6422 cm^{-1}. Finally, the **aC** band at 3268 cm^{-1} decreases and increases upon irradiation at 6378 and at 6405 cm^{-1}, respectively.

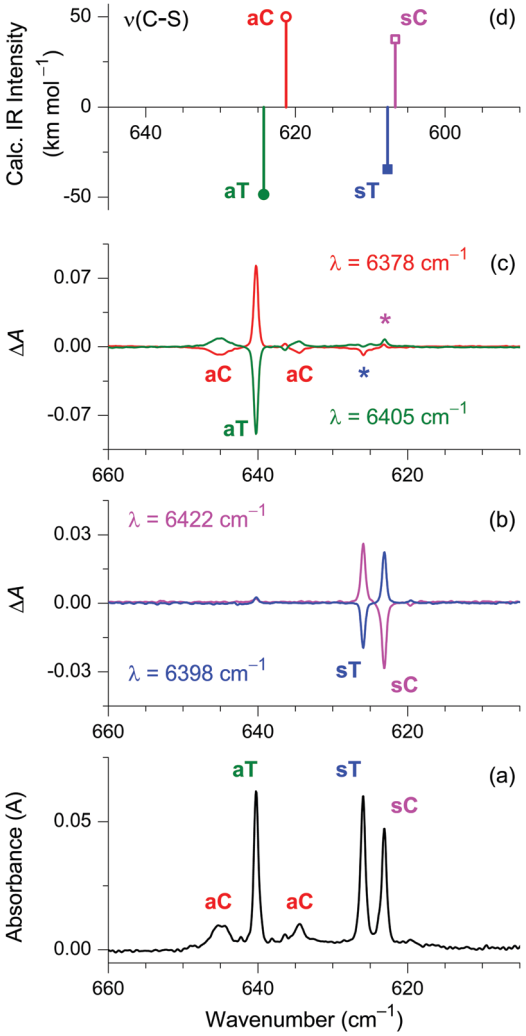

Fig. 5 (a) Experimental mid-IR spectrum, showing the new bands of imino-thiol photoproducts growing upon UV irradiation of thioacetamide isolated in an argon matrix at 11 K; experimental difference spectra showing changes in absorption (ΔA) upon subsequent irradiation of the sample with near-IR light (b) at 6398 cm^{-1} (blue) or at 6422 cm^{-1} (pink); and (c) at 6405 cm^{-1} (green) or at 6378 cm^{-1} (red); (d) anharmonic wavenumbers (unscaled) and IR intensities due to ν(C–S) modes of **sC** (pink, open squares) and **sT** (blue, closed squares), and **aT** (green, closed circles) and **aC** (red, open circles) imino-thiol forms computed at the B3LYP/6-311++G(3df,3pd) level of theory. The intensities of the **sT** and **aT** forms are multiplied by (−1). The bands in frame (**c**) designated by asterisks are due to residual conformational changes of the *syn*-forms (**sC** and **sT**) induced by the unfiltered light of the spectrometer source.

3.2.4. 1300–1200 cm^{-1} region. Fig. 7 shows the spectral region of 1300–1200 cm^{-1}. Only one fundamental transition,

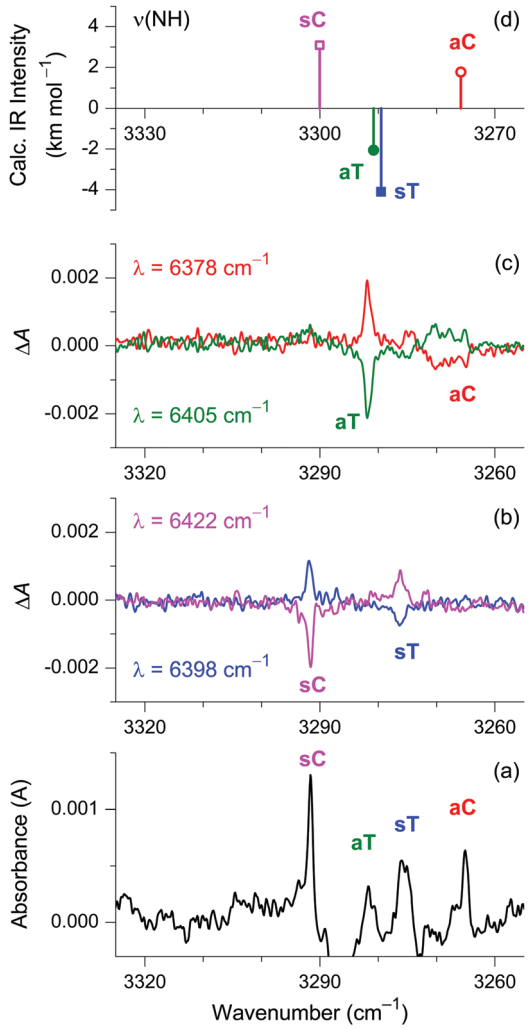

Fig. 6 (a) Experimental mid-IR spectrum, showing the new bands of imino-thiol photoproducts growing upon UV irradiation of thioacetamide isolated in an argon matrix at 11 K; experimental difference spectra showing changes in absorption (ΔA) upon subsequent irradiation of the sample with near-IR light (b) at 6398 cm^{-1} (blue) or at 6422 cm^{-1} (pink); and (c) at 6405 cm^{-1} (green) or at 6378 cm^{-1} (red); (d) anharmonic wavenumbers (unscaled) and IR intensities due to ν(NH) modes of **sC** (pink, open squares) and **sT** (blue, closed squares), and **aT** (green, closed circles) and **aC** (red, open circles) imino-thiol forms computed at the B3LYP/6-311++G(3df,3pd) level of theory. The intensities of the **sT** and **aT** forms are multiplied by (−1).

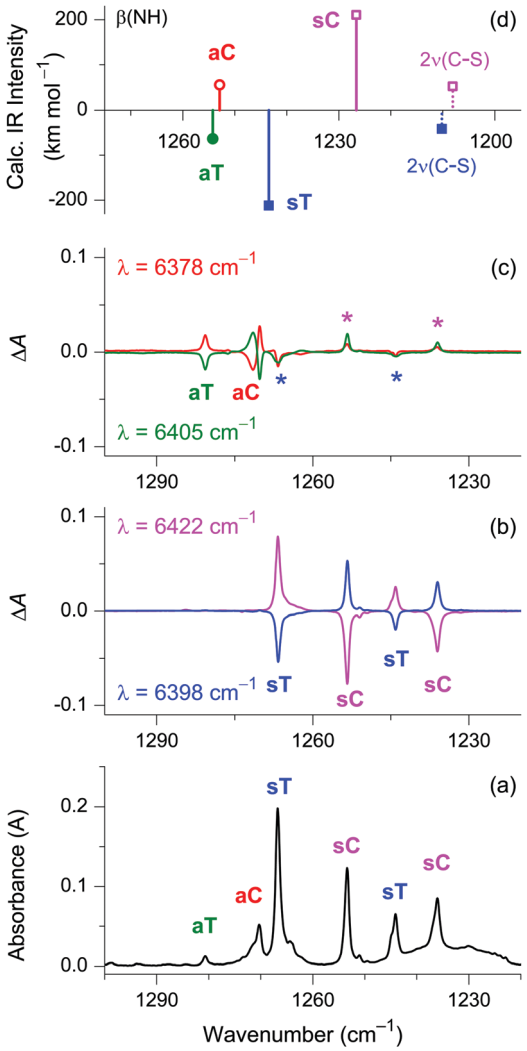

Fig. 7 (a) Experimental mid-IR spectrum, showing the new bands of imino-thiol photoproducts growing upon UV irradiation of thioacetamide isolated in an Ar matrix at 11 K; experimental difference spectra showing changes in absorption (ΔA) upon subsequent irradiation of the sample with near-IR light (b) at 6398 cm^{-1} (blue) or at 6422 cm^{-1} (pink); and (c) at 6405 cm^{-1} (green) or at 6378 cm^{-1} (red); (d) anharmonic wavenumbers (unscaled) and IR intensities of **sC** (pink, open squares) and **sT** (blue, closed squares), and **aT** (green, closed circles) and **aC** (red, open circles) imino-thiol forms computed at the B3LYP/6-311++G(3df,3pd) level of theory. Only transitions due to the β(NH) and 2ν(C–S) modes appear in this range. The computed anharmonic IR intensities due to the 2ν(C–S) vibrations were multiplied by 3, for the **sT** and **sC** forms. The computed intensities due to the **sT** and **aT** forms were additionally multiplied by (−1). The bands in frame (**c**) designated by asterisks are due to residual conformational changes of the *syn*-forms (**sC** and **sT**) induced by the unfiltered light of the spectrometer source.

i.e., the β(NH) bending mode, was formerly assigned to each isomer in this range of the spectrum.[3] Yet, two pairs of bands were observed in the experimental spectra, which are ascribable to each of the **sC** and **sT** forms. The assignment of these bands was made possible taking into account the results of the performed anharmonic computations as well as those resulting from the near-IR irradiation experiments. The vibrational bands at 1254 and 1236 cm^{-1} decrease upon irradiation at 6422 cm^{-1} and increase during irradiation at 6398 cm^{-1}, therefore they undoubtedly belong to the **sC** isomer. In contrast, the signals at 1267 and 1244 cm^{-1} behave in the opposite way, *i.e.* increase and decrease when the sample is irradiated at 6422 and 6398 cm^{-1}, respectively, thus they can be safely assigned to the **sT** isomer. The higher-frequency band in each pair may be assigned to the β(NH) bending mode, whose calculated frequencies (1227 and 1243 cm^{-1} for **sC** and **sT**, respectively) closely match the experimental values. The β(NH) modes of the *anti* isomers can be found at 1272 (**aC**) and 1281 cm^{-1} (**aT**); the computed values are 1253 and 1254 cm^{-1}, respectively. On the basis of the anharmonic computations, it was also possible to

give the alternative explanation that the bands appearing at lower frequencies (the lower IR intensity bands at 1236 and 1244 cm^{-1}) are not due to the β(NH) bending fundamental mode (as suggested previously)[3] but could be ascribed to the 2ν(C–S) first stretching overtone transition instead (computed values: 1208 and 1210 cm^{-1} for **sC** and **sT**, respectively).

3.2.5. 1090–1010 cm^{-1} region. Fig. 8 (see also Tables 2 and 3) shows that the frequency of the $\rho(CH_3)$ rocking mode of **aC** (with A′ symmetry) is predicted by the computations to coincide with that of the $\rho(CH_3)$ rocking mode of **aT** (with A″ symmetry), and *vice versa*. Given the fact that the bands of both A″ $\rho(CH_3)$ rocking modes are much weaker in the IR spectrum than those of the corresponding modes of A′ symmetry, this would imply that the experimental spectrum should show only one pair of bands affected by the performed near-IR irradiation. Somewhat surprisingly, the experiment shows two pairs of bands. The doublet with maxima at 1050 and 1047 cm^{-1} is assigned to the modes with A′ symmetry, while a second, lower intensity doublet with maxima at 1037 and 1036 cm^{-1} is here tentatively assigned to those with A″ symmetry. Yet another band, showing behavior typical of the **aT** form (a decrease/increase upon irradiation at 6405 and 6387 cm^{-1}, respectively), near 1072 cm^{-1}, is also observed in the spectrum. This band cannot be ascribed to any of the predicted fundamental, overtone, or combination modes of any of the four thiol forms. The carrier of this band is unclear and needs further investigation. The $\rho(CH_3)$ rocking modes for **sC** and **sT** with A′ symmetry can be found at 1070 and 1063 cm^{-1} (computed values 1058 and 1054 cm^{-1}), respectively. Those with A″ symmetry are found at 1042 (**sC**) and 1043/1041 cm^{-1} (doublet, **sT**), with a theoretical value of 1042 cm^{-1} for both isomers.

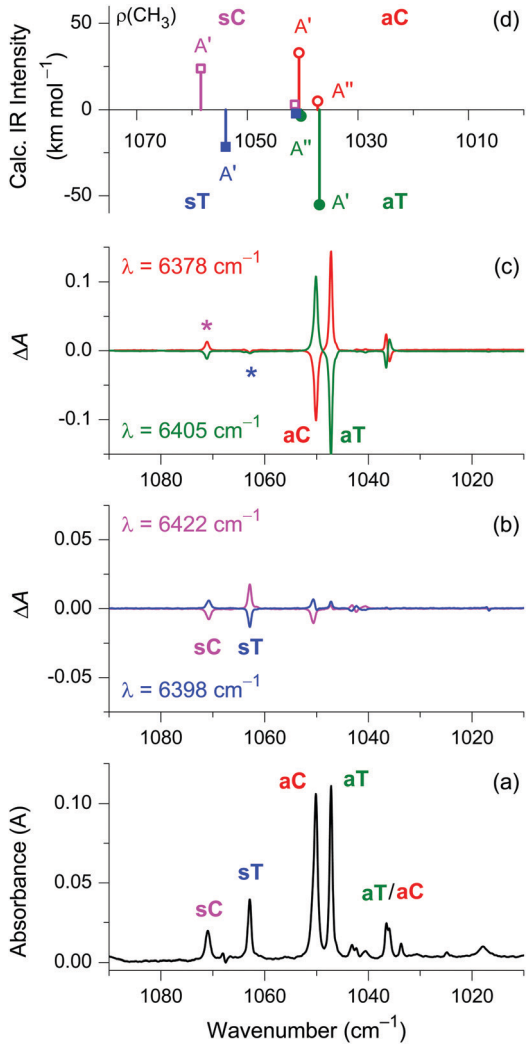

Fig. 8 (a) Experimental mid-IR spectrum, showing the new bands of imino-thiol photoproducts growing upon UV irradiation of thioacetamide isolated in an Ar matrix at 11 K; experimental difference spectra showing changes in absorption (ΔA) upon subsequent irradiation of the sample with near-IR light (b) at 6398 cm^{-1} (blue) or at 6422 cm^{-1} (pink); and (c) at 6405 cm^{-1} (green) or at 6378 cm^{-1} (red); (d) anharmonic wavenumbers (unscaled) and IR intensities of **sC** (pink, open squares) and **sT** (blue, closed squares), and **aT** (green, closed circles) and **aC** (red, open circles) imino-thiol forms computed at the B3LYP/6-311++G(3df,3pd) level of theory. The intensities of the **sT** and **aT** forms are multiplied by (−1). Only transitions due to the $\rho(CH_3)$ modes appear in this range. The A′ or A″ labels designate the $\rho(CH_3)$ modes of the corresponding symmetry. The bands in frame (c) designated by asterisks are due to residual conformational changes of the *syn*-forms (**sC** and **sT**) induced by the unfiltered light of the spectrometer source.

3.3. Kinetics of near-IR irradiation and quantum yields

The kinetics of the transformations was also monitored on line during the irradiation experiments performed in Budapest. Fig. 9 visualizes the results. In order to fit the decay profiles, a single exponential decay function was used:

$$A_t(sX, \nu_y) = A_{t=0}(sX, \nu_y)e^{-kt} + A_{t=\infty}(sX, \nu_y) \quad (1)$$

where $A_t(\nu X)$ is the integrated area (in cm^{-1}) of the band ν_y of conformer xX (x = **a** or **s**, X = **C** or **T**; y = 816 cm^{-1} if xX = **aC**, y = 818 cm^{-1} if xX = **aT**, y = 836 cm^{-1} if xX = **sC** and y = 849 cm^{-1} if xX = **sT**), t is time (in min), and k is the first-order rate constant (in min^{-1}). $t_{1/2}$ is the half-life (in min) of the decaying isomer, which can be calculated as follows:

$$t_{1/2} = \frac{\ln 2}{k} \quad (2)$$

The following equation was used to fit the growth profiles:

$$A_t(sX, \nu_y) = A_{t=\infty}(sX, \nu_y)(1 - e^{-kt}) \quad (3)$$

Table 7 summarizes the decay/growth rates determined by using the functions described in eqn (1) and (3). It is important to note that the processes induced by near-IR irradiation are significantly faster (half-lives of approximately 10 minutes) than those of the spontaneous tunneling previously reported (approximately 80 and 50 minutes for the **sC** to **sT** conversion process when using the 870 cm^{-1} filter and when exposed to the broadband IR radiation of the FT-IR spectrometer source, respectively).[4] The reverse process (*i.e.*, **sT** to **sC**) was also found to be easily induced by exciting the 2ν(NH) first stretching overtone of **sT**. Also, unlike in the completely unperturbed system (*i.e.*, when the spectrometer source is blocked),[4] the conversion between the *anti* forms could easily be achieved in the present near-IR irradiation experiments. Furthermore, the **aT** to **aC**

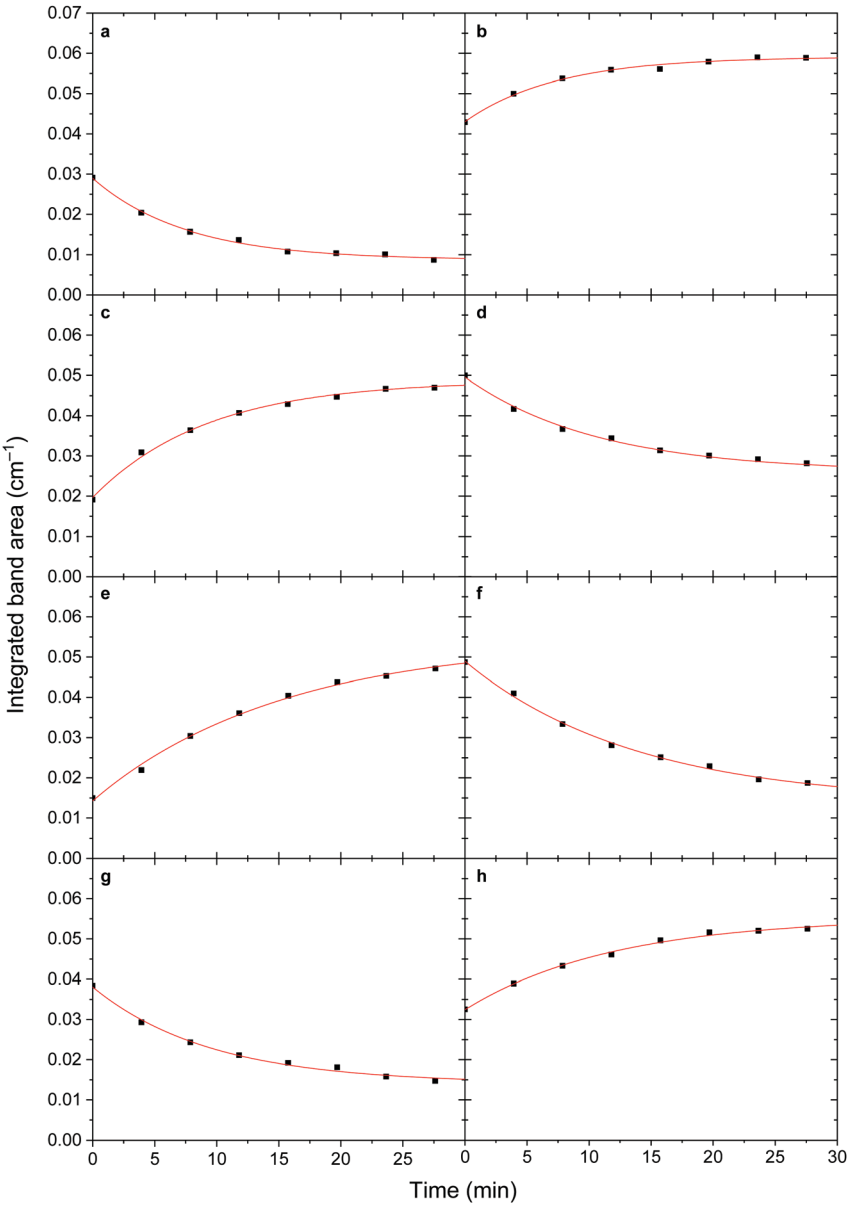

Fig. 9 (a) Kinetic growth of the band at 816 cm^{-1} (**aC**) and (b) decay of the band at 818 cm^{-1} (**aT**) during the near-IR irradiation at 6405 cm^{-1}; (c) kinetic decay of the band at 816 cm^{-1} (**aC**) and (d) kinetic growth of the band at 818 cm^{-1} (**aT**) during the near-IR irradiation at 6378 cm^{-1}; (e) kinetic decay of the band at 836 cm^{-1} (**sC**) and (f) kinetic growth of the band at 849 cm^{-1} (**sT**) during the near-IR irradiation at 6422 cm^{-1}; (g) kinetic growth of the band at 836 cm^{-1} (**sC**) and (h) kinetic decay of the band at 849 cm^{-1} (**sT**) during the near-IR irradiation at 6398 cm^{-1}.

Table 7 Kinetic decay/growth rates upon near-IR irradiation ($k_{\mathbf{x}}$, in min^{-1}, where **x** denotes one of the four thiol isomers). Positive values indicate growth, whereas the negative signs show decay. Kinetic half-lives ($t_{1/2}$, in min) of the decaying isomer calculated from the respective $k_{\mathbf{x}}$ values are also given

	Near-IR irrad. (cm^{-1})			
	6405	6378	6422	6398
$k_{\mathbf{aC}}$	$(4.6 \pm 0.5) \times 10^{-2}$	$-(7.3 \pm 0.8) \times 10^{-2}$	—	—
$k_{\mathbf{aT}}$	$-(5.1 \pm 0.4) \times 10^{-2}$	$(5.8 \pm 0.6) \times 10^{-2}$	—	—
$k_{\mathbf{sC}}$	—	—	$-(9.2 \pm 0.7) \times 10^{-2}$	$(7.5 \pm 0.4) \times 10^{-2}$
$k_{\mathbf{sT}}$	—	—	$(9.3 \pm 1.0) \times 10^{-2}$	$-(6.5 \pm 0.4) \times 10^{-2}$
$t_{1/2}$	13.7 ± 1.2	9.5 ± 1.0	7.5 ± 0.6	10.7 ± 0.6

process occurs an order of magnitude more rapidly than when the thiols are simply exposed to broadband IR radiation of the spectrometer source (*cf.* half-lives of approximately 10 and 170 minutes, respectively).[4]

Table 8 Quantum yields for the SH rotamerization induced by the excitation of the 2ν(NH) stretching overtones of the thiol conformers

	Near-IR irrad. (cm^{-1})			
	6405 (**aT**)	6378 (**aC**)	6422 (**sC**)	6398 (**sT**)
A_{int}[a] (cm)	0.0531	0.0393	0.0274	0.0487
α[a] (cm)	8.8×10^{-18}	8.6×10^{-18}	8.8×10^{-18}	8.3×10^{-18}
N (cm^{-2})	6.9×10^{15}	5.3×10^{15}	3.6×10^{15}	6.8×10^{15}
A	2.5×10^{-4}	2.9×10^{-4}	1.3×10^{-4}	2.4×10^{-4}
$\sigma^i(\nu)$ (eqn (1)) (cm^2)	3.6×10^{-20}	5.4×10^{-20}	3.6×10^{-20}	3.5×10^{-20}
P (W)	0.110	0.114	0.110	0.114
E_{photon} (J)	1.3×10^{-19}	1.3×10^{-19}	1.3×10^{-19}	1.3×10^{-19}
$I(\nu)$	4.2×10^{17}	4.4×10^{17}	4.2×10^{17}	4.4×10^{17}
$\phi(i)$ (eqn (4))	5.6×10^{-2}	5.1×10^{-2}	1.0×10^{-1}	7.0×10^{-2}
N_{iso}	1.2×10^{13}	1.3×10^{13}	1.1×10^{13}	1.5×10^{13}
N_{abs}	4.8×10^{14}	5.9×10^{14}	2.5×10^{14}	4.9×10^{14}
$\phi(i)$ (eqn (6))	2.5×10^{-2}	2.2×10^{-2}	4.4×10^{-2}	3.1×10^{-2}
$\phi(i)_{mean}$	$(4.1 \pm 1.6) \times 10^{-2}$	$(3.7 \pm 1.5) \times 10^{-2}$	$(7.2 \pm 2.8) \times 10^{-2}$	$(5.1 \pm 2.0) \times 10^{-2}$

[a] Values of the τ(NH) vibrational modes of the respective thiol conformers.

The quantum yields of the studied processes may be also estimated using the formula described in ref. 43, 47 and 52:

$$\phi(i) = \frac{k_p(\tilde{\nu})}{\sigma^i(\tilde{\nu}) I(\tilde{\nu})} \quad (4)$$

where $\phi(i)$ is the quantum yield of the rotamerization by exciting vibrational mode i, $k_p(\tilde{\nu})$ (in s^{-1}) is the rotamerization rate upon irradiating at a wavenumber $\tilde{\nu}$ (Table 8), $\sigma^i(\tilde{\nu})$ (in cm^2) is the absorption cross-section of vibrational mode i at the excitation frequency $\tilde{\nu}$, and I (in s^{-1} cm^{-2}) is the averaged photon intensity of the laser beam. $\sigma^i(\tilde{\nu})$ can be obtained by dividing the absorbance of the excited peak (A, dimensionless value) by the calculated column density (N, in cm^{-2}) of the decaying conformer at the beginning of the irradiation, whereas the latter can be derived from the integrated peak area (A_{int}, in cm) of one absorption band of the conformer and by knowing the absorption coefficient (α, in cm) and the area of irradiation (S = 2 cm^2) of that absorption:

$$N = \ln(10)\frac{A_{int}}{\alpha S} \quad (5)$$

Although α is unknown, it can be estimated from the computed anharmonic IR intensities (Tables S2–S6, ESI†); for calculating N, the τ(NH) torsional vibrational modes of the imino-thiol forms in the mid-IR region of 860–800 cm^{-1} were chosen, since they are well-separated and have relatively high intensity. The value of I can be calculated by dividing the output power of the produced near-IR laser light (P, in W) by the photon energy (E_{photon}, in J) and by 2 cm^2 (*i.e.*, the value of S).

Alternatively, $\phi(i)$ can also be calculated from:

$$\phi(i) = \frac{N_{iso}}{N_{abs}} \quad (6)$$

where N_{iso} is the number of molecules converted and N_{abs} is the number of photons absorbed per time unit (both in s^{-1}).

$$N_{iso} = k_p(\tilde{\nu}) N S \quad (7)$$

$$N_{abs} = (1 - 10^{-A}) I S \quad (8)$$

The averaged value of $\phi(i)$ ($\phi(i)_{mean}$, varying between 3.7 and 7.2 $\times$ 10^{-2}) is comparable to the quantum yields obtained when excitation was performed using the 2ν(OH) first stretching overtones for molecules like formic acid ($\phi(i)$ = 1.7 $\times$ 10^{-1} and 7 $\times$ 10^{-2}, respectively),[47] acetic acid (2.2 $\times$ 10^{-2}),[52] and propionic acid (1.4 $\times$ 10^{-2}),[43] but considerably higher than those of glycine (8 $\times$ 10^{-4}) and alanine (5 $\times$ 10^{-4} and 1 $\times$ 10^{-3}, respectively).[70,71] Note that the majority of earlier studies used direct excitation of the group which undergoes isomerization while the present work utilizes a remote molecular antenna to induce conformational change in other parts of the molecule. The relative uncertainty of $\phi(i)_{mean}$ is about 50%, which also agrees with those previously determined.[43,52] It is important to note that in each of the aforementioned cases (including the present work, Fig. 4), the excitation energy was above the rotamerization barrier.

4. Conclusions

Thioacetamide was isolated in argon matrices at low temperature and studied by means of FT-IR spectroscopy. After deposition, only the more stable **Tn** tautomeric form is present in the sample. This form could be then converted to the thiol tautomeric forms by *in situ* narrowband UV irradiation. The four imino-thiol isomers (**aC**, **aT**, **sC** and **sT**) were generated. These isomers give rise to distinctive 2ν(NH) first stretching overtone bands in the 6400 cm^{-1} spectral region and, upon exposing these forms to near-IR light with a frequency matching their respective vibrational band, selective and reversible rotamerizations between them could be successfully induced. In particular, interconversions of the (**aC**, **aT**) and (**sC**, **sT**) pairs of isomers (corresponding to thiol group internal rotation about the C–S bond) were promoted, while no isomerization within the imino fragment was observed. This constitutes the first example of an imino group used as a vibrational antenna for controlling molecular conformations. The rotamerization processes could be followed by the changes they originate throughout the mid-IR spectra, allowing us to perform unequivocal vibrational assignments for all four thiol forms (and also for the **Tn** tautomer), extending the previously reported data.[3,4]

The irradiation experiments were supplemented by quantum chemical computations, which also helped in the assignment of

the spectra. When comparing the theoretical and experimental vibrational frequencies of the thioacetamide isomers, it could be noticed that the agreement between the two sets of data is good in general, the same applying also to the IR intensities. This good reproduction of the experimental data by the theoretical computations confirmed the interpretation of the observed spectra and gave further support to the performed assignments. An interesting observation that deserves to be mentioned is the fact that the intensities of the 2ν(NH) first stretching overtones of the imino-thiol forms of thioacetamide are comparable to those of the corresponding ν(NH) stretching fundamentals. This is the first time that such a phenomenon is reported for an imine molecule. Considering that for matrix-isolated molecules the infrared intensities of the bands due to fundamental –NH stretching modes are about an order of magnitude higher than those of the corresponding first stretching overtones,[80,81] the observation of the present study can be interpreted in two ways: either the intensities of the 2ν(NH) first stretching overtones are abnormally high, or the intensities of the ν(NH) stretching fundamentals are abnormally low. The analysis of the available bibliographic data for molecules having –NH or $-NH_2$ groups indicates that the second explanation is correct. The typical computed infrared intensities of the ν(NH) and 2ν(NH) modes fall in the ranges 50–70 km mol^{-1} and 2–6 km mol^{-1}, respectively.[80] Thus, in the present study we found that all imino-thiol isomers have unusually low infrared intensities of the fundamental NH stretching modes.

The kinetics of the irradiation processes were also monitored *in situ*, demonstrating that the selective rotamerizations induced by near-IR irradiation are significantly faster than the previously reported spontaneous processes occurring in this system. Quantum yields were also estimated, showing that they are comparable with those of several carboxylic acids previously studied, while higher than for the amino acids glycine and alanine, which appears as an interesting subject for future investigation. It must be pointed out that the quantum yield values are comparable despite the fact that this study uses a remote molecular antenna for vibrational excitation relative to the group undergoing the conformational change, unlike the majority of earlier studies, which utilized the direct excitation of the first stretching OH overtone (2νOH) in order to induce conformational changes of the same –OH group.

Conflicts of interest

There are no conflicts to declare.

Acknowledgements

This work was supported by Project POCI-01-0145-FEDER-016617 and Project POCI-01-0145-FEDER-028973, funded by FEDER *via* Portugal 2020 – POCI, and by National Funds *via* the Portuguese Foundation for Science and Technology (FCT). The Coimbra Chemistry Centre is supported by the FCT through the project UID/QUI/0313/2019, cofounded by COMPETE. S. G. acknowledges the European Union's Horizon 2020 research and innovation programme under grant agreement number 654148 (LaserLab Europe) and project CENTRO-01-0145-FEDER-022124 (LLPT: LaserLab-Portugal) funded by FEDER *via* CENTRO 2020, and by National Funds *via* FCT. C. M. N. and I. R. acknowledge the FCT for an Auxiliary Researcher grant and an Investigador FCT grant, respectively. I. P. C. and G. T. acknowledge the support of the Lendület program of the Hungarian Academy of Sciences. This work was completed within the framework of the ELTE Excellence Program (1783-3/2018/FEKUTSTRAT) supported by the Hungarian Ministry of Human Capacities (EMMI).

References

1 E. Spinner, *Spectrochim. Acta*, 1959, **15**, 95–109.
2 M. E. Jacox and D. E. Milligan, *J. Mol. Spectrosc.*, 1975, **58**, 142–157.
3 L. Lapinski, H. Rostkowska, A. Khvorostov and M. J. Nowak, *Phys. Chem. Chem. Phys.*, 2003, **5**, 1524–1529.
4 S. Góbi, C. M. Nunes, I. Reva, G. Tarczay and R. Fausto, *Phys. Chem. Chem. Phys.*, 2019, **21**, 17063–17071.
5 R. A. Linke, M. A. Frerking and P. Thaddeus, *Astrophys. J.*, 1979, **234**, L139–L142.
6 L. Kolesniková, B. Tercero, J. Cernicharo, J. L. Alonso, A. M. Daly, B. P. Gordon and S. T. Shipman, *Astrophys. J., Lett.*, 2014, **784**, L7.
7 H. S. P. Müller, A. Belloche, L.-H. Xu, R. M. Lees, R. T. Garrod, A. Walters, J. van Wijngaarden, F. Lewen, S. Schlemmer and K. M. Menten, *Astron. Astrophys.*, 2016, **587**, A92.
8 R. L. Hudson, *Phys. Chem. Chem. Phys.*, 2016, **18**, 25756–25763.
9 S. Pavithraa, R. R. J. Methikkalam, P. Gorai, J.-I. Lo, A. Das, B. N. Raja Sekhar, T. Pradeep, B.-M. Cheng, N. J. Mason and B. Sivaraman, *Spectrochim. Acta, Part A*, 2017, **178**, 166–170.
10 S. Pavithraa, D. Sahu, G. Seth, J.-I. Lo, B. N. Raja Sekhar, B.-M. Cheng, A. Das, N. J. Mason and B. Sivaraman, *Astrophys. Space Sci.*, 2017, **362**, 126.
11 R. L. Hudson and P. A. Gerakines, *Astrophys. J.*, 2018, **867**, 138.
12 P. Gorai, An. Das, Am. Das, B. Sivaraman, E. E. Etim and S. K. Chakrabarti, *Astrophys. J.*, 2017, **836**, 70.
13 A. Maris, C. Calabrese, L. B. Favero, L. Evangelisti, I. Usabiaga, S. Mariotti, C. Codella, L. Podio, N. Balucani, C. Ceccarelli, B. LeFloch and S. Melandri, *ACS Earth Space Chem.*, 2019, **3**, 1537–1549.
14 B. A. McGuire, C. N. Shingledecker, E. R. Willis, K. L. K. Lee, M.-A. Martin-Drumel, G. A. Blake, C. L. Brogan, A. M. Burkhardt, P. Caselli, K.-J. Chuang, S. El-Abd, T. R. Hunter, S. Ioppolo, H. Linnartz, A. J. Remijan, C. Xue and M. C. McCarthy, *Astrophys. J.*, 2019, **883**, 201.
15 B. Noszál, D. Visky and M. Kraszni, *J. Med. Chem.*, 2000, **43**, 2176–2182.
16 H. Li and G. J. Thomas, Jr, *J. Am. Chem. Soc.*, 1991, **113**, 456–462.
17 A. R. Buller and C. A. Townsend, *Proc. Natl. Acad. Sci. U. S. A.*, 2013, **110**, E653–E661.

18 M. Kurien, A. P. Susamma and A. P. Kuriakose, *Prog. Rubber, Plast. Recycl. Technol.*, 2004, **20**, 133–162.
19 NTP (National Toxicology Program). 2016. Report on Carcinogens, Fourteenth Edition: Thioacetamide; Research Triangle Park, NC: U.S. Department of Health and Human Services, Public Health Service. https://ntp.niehs.nih.gov/go/roc14.
20 A. Dasgupta, R. Chatterjee and J. R. Chowdhury, *Oncology*, 1981, **38**, 249–253.
21 C.-N. Yeh, A. Maitra, K.-F. Lee, Y.-Y. Jan and M.-F. Chen, *Carcinogenesis*, 2004, **25**, 631–636.
22 IARC (International Agency for Research on Cancer). 1974. Thioacetamide. In: Some Anti-thyroid and Related Substances, Nitrofurans and Industrial Chemicals. IARC Monographs on the Evaluation of Carcinogenic Risk of Chemicals to Man, vol. 7. Lyon, France: IARC, 77–83.
23 Y.-C. Zhang, H. Wang, B. Wang, H. Yan and M. Yoshimura, *J. Cryst. Growth*, 2002, **243**, 214–217.
24 C. M. Liddell and C. J. Summers, *J. Colloid Interface Sci.*, 2004, **274**, 103–106.
25 Z.-P. Liu, J.-B. Liang, D. Xu, J. Lu and Y.-T. Qian, *Chem. Commun.*, 2004, 2724–2725.
26 Y. Jin, Y.-H. Zhu, X.-L. Yang., H.-B. Jiang and C.-Z. Li, *J. Colloid Interface Sci.*, 2006, **301**, 130–136.
27 L. Yang, R.-M. Xing, Q.-M. Shen, K. Jiang, F. Ye, J.-Y. Wang and Q.-S. Ren, *J. Phys. Chem. B*, 2006, **110**, 10534–10539.
28 G.-J. Zhou, M.-K. Lü, Z.-L. Xiu, S.-F. Wang, H.-P. Zhang, Y.-Y. Zhou and S.-M. Wang, *J. Phys. Chem. B*, 2006, **110**, 6543–6548.
29 R. Knudsen, O. Sala and Y. Hase, *J. Mol. Struct.*, 1994, **321**, 197–203.
30 M. J. Nowak, L. Lapinski, H. Rostkowska, A. Leś and L. Adamowicz, *J. Phys. Chem.*, 1990, **94**, 7406–7414.
31 M. J. Nowak, L. Lapinski, J. Fulara, A. Leś and L. Adamowicz, *J. Phys. Chem.*, 1991, **95**, 2404–2411.
32 D. Prusinowska, L. Lapinski, M. J. Nowak and L. Adamowicz, *Spectrochim. Acta, Part A*, 1995, **51**, 1809–1826.
33 E. M. Brás and R. Fausto, *J. Mol. Struct.*, 2018, **1172**, 42–54.
34 E. M. Brás and R. Fausto, *J. Photochem. Photobiol., A*, 2018, **357**, 185–192.
35 H. Rostkowska, L. Lapinski and M. J. Nowak, *J. Phys. Org. Chem.*, 2010, **23**, 56–66.
36 H. Rostkowska, L. Lapinski, I. Reva, B. J. A. N. Almeida, M. J. Nowak and R. Fausto, *J. Phys. Chem. A*, 2011, **115**, 12142–12149.
37 L. Lapinski, M. J. Nowak, R. Kołos, J. S. Kwiatkowski and J. Leszczyński, *Spectrochim. Acta, Part A*, 1998, **54**, 685–693.
38 H. Rostkowska, L. Lapinski and M. J. Nowak, *J. Phys. Chem. A*, 2003, **107**, 804–809.
39 L. Lapinski, H. Rostkowska, A. Khvorostov, M. Yaman, R. Fausto and M. J. Nowak, *J. Phys. Chem. A*, 2004, **108**, 5551–5558.
40 H. Rostkowska, L. Lapinski, A. Khvorostov and M. J. Nowak, *J. Phys. Chem. A*, 2003, **107**, 6373–6380.
41 H. Rostkowska, L. Lapinski and M. J. Nowak, *Phys. Chem. Chem. Phys.*, 2018, **20**, 13994–14002.
42 E. M. S. Maçôas, L. Khriachtchev, M. Pettersson, J. Lundell, R. Fausto and M. Räsänen, *Vib. Spectrosc.*, 2004, **34**, 73–82.
43 E. M. S. Maçôas, L. Khriachtchev, M. Pettersson, R. Fausto and M. Räsänen, *Phys. Chem. Chem. Phys.*, 2005, **7**, 743–749.
44 L. Khriachtchev, *J. Mol. Struct.*, 2008, **880**, 14–22.
45 M. Pettersson, J. Lundell, L. Khriachtchev and M. Räsänen, *J. Am. Chem. Soc.*, 1997, **119**, 11715–11716.
46 M. Pettersson, E. M. S. Maçôas, L. Khriachtchev, J. Lundell, R. Fausto and M. Räsänen, *J. Chem. Phys.*, 2002, **117**, 9095–9098.
47 E. M. S. Maçôas, L. Khriachtchev, M. Pettersson, J. Juselius, R. Fausto and M. Räsänen, *J. Chem. Phys.*, 2003, **119**, 11765–11772.
48 K. Marushkevich, L. Khriachtchev, J. Lundell and M. Räsänen, *J. Am. Chem. Soc.*, 2006, **128**, 12060–12061.
49 K. Marushkevich, L. Khriachtchev, J. Lundell, A. Domanskaya and M. Räsänen, *J. Phys. Chem. A*, 2010, **114**, 3495–3502.
50 E. M. S. Maçôas, L. Khriachtchev, M. Pettersson, R. Fausto and M. Räsänen, *J. Am. Chem. Soc.*, 2003, **125**, 16188–16189.
51 E. M. S. Maçôas, L. Khriachtchev, R. Fausto and M. Räsänen, *J. Phys. Chem. A*, 2004, **108**, 3380–3389.
52 E. M. S. Maçôas, L. Khriachtchev, M. Pettersson, R. Fausto and M. Räsänen, *J. Chem. Phys.*, 2004, **121**, 1331–1338.
53 E. M. S. Maçôas, L. Khriachtchev, M. Pettersson, R. Fausto and M. Räsänen, *J. Phys. Chem. A*, 2005, **109**, 3617–3625.
54 I. Reva, C. M. Nunes, M. Biczysko and R. Fausto, *J. Phys. Chem. A*, 2015, **119**, 2614–2627.
55 E. M. S. Maçôas, R. Fausto, M. Pettersson, L. Khriachtchev and M. Räsänen, *J. Phys. Chem. A*, 2000, **104**, 6956–6961.
56 E. M. S. Maçôas, R. Fausto, J. Lundell, M. Pettersson, L. Khriachtchev and M. Räsänen, *J. Phys. Chem. A*, 2000, **104**, 11725–11732.
57 E. M. S. Maçôas, R. Fausto, J. Lundell, M. Pettersson, L. Khriachtchev and M. Räsänen, *J. Phys. Chem. A*, 2001, **105**, 3922–3933.
58 A. Halasa, L. Lapinski, I. Reva, H. Rostkowska, R. Fausto and M. J. Nowak, *J. Phys. Chem. A*, 2014, **118**, 5626–5635.
59 A. Halasa, L. Lapinski, H. Rostkowska, I. Reva and M. J. Nowak, *J. Phys. Chem. A*, 2015, **119**, 2203–2210.
60 R. F. G. Apóstolo, G. Bazsó, R. R. F. Bento, G. Tarczay and R. Fausto, *J. Mol. Struct.*, 2016, **1125**, 288–295.
61 R. F. G. Apóstolo, R. R. F. Bento and R. Fausto, *Croat. Chem. Acta*, 2015, **88**, 377–386.
62 R. F. G. Apóstolo, G. Bazsó, G. Ogruc-Ildiz, G. Tarczay and R. Fausto, *J. Chem. Phys.*, 2018, **148**, 044303.
63 G. Bazsó, S. Góbi and G. Tarczay, *J. Phys. Chem. A*, 2012, **116**, 4823–4832.
64 C. Araujo-Andrade, I. Reva and R. Fausto, *J. Chem. Phys.*, 2014, **140**, 064306.
65 L. Lapinski, I. Reva, H. Rostkowska, A. Halasa, R. Fausto and M. J. Nowak, *J. Phys. Chem. A*, 2013, **117**, 5251–5259.
66 A. Halasa, L. Lapinski, I. Reva, H. Rostkowska, R. Fausto and M. J. Nowak, *J. Phys. Chem. A*, 2015, **119**, 1037–1047.
67 A. Halasa, I. Reva, L. Lapinski, M. J. Nowak and R. Fausto, *J. Phys. Chem. A*, 2016, **120**, 2078–2088.
68 N. Kuş and R. Fausto, *J. Chem. Phys.*, 2017, **146**, 124305.
69 J. P. Wagner, H. P. Reisenauer, V. Hirvonen, C.-H. Wu, J. L. Tyberg, W. D. Allen and P. R. Schreiner, *Chem. Commun.*, 2016, **52**, 7858–7861.

70 G. Bazsó, G. Magyarfalvi and G. Tarczay, *J. Phys. Chem. A*, 2012, **116**, 10539–10547.
71 G. Bazsó, E. E. Najbauer, G. Magyarfalvi and G. Tarczay, *J. Phys. Chem. A*, 2013, **117**, 1952–1962.
72 C. M. Nunes, L. Lapinski, R. Fausto and I. Reva, *J. Chem. Phys.*, 2013, **138**, 125101.
73 E. E. Najbauer, G. Bazsó, S. Góbi, G. Magyarfalvi and G. Tarczay, *J. Phys. Chem. B*, 2014, **118**, 2093–2103.
74 E. E. Najbauer, G. Bazsó, R. Apóstolo, R. Fausto, M. Biczysko, V. Barone and G. Tarczay, *J. Phys. Chem. B*, 2015, **119**, 10496–10510.
75 L. Lapinski, M. J. Nowak, I. Reva, H. Rostkowska and R. Fausto, *Phys. Chem. Chem. Phys.*, 2010, **12**, 9615–9618.
76 I. Reva, M. J. Nowak, L. Lapinski and R. Fausto, *J. Chem. Phys.*, 2012, **136**, 064511.
77 L. Lapinski, I. Reva, H. Rostkowska, R. Fausto and M. J. Nowak, *J. Phys. Chem. B*, 2014, **118**, 2831–2841.
78 A. Sharma, I. Reva and R. Fausto, *J. Am. Chem. Soc.*, 2009, **131**, 8752–8753.
79 G. Bazsó, G. Magyarfalvi and G. Tarczay, *J. Mol. Struct.*, 2012, **1025**, 33–42.
80 A. J. Lopes Jesus, I. Reva, C. Araujo-Andrade and R. Fausto, *J. Am. Chem. Soc.*, 2015, **137**, 14240–14243.
81 A. J. Lopes Jesus, R. Fausto and I. Reva, *J. Phys. Chem. A*, 2017, **121**, 3372–3382.
82 A. Halasa, I. Reva, L. Lapinski, H. Rostkowska, R. Fausto and M. J. Nowak, *J. Phys. Chem. A*, 2016, **120**, 2647–2656.
83 B. Kovács, N. Kuş, G. Tarczay and R. Fausto, *J. Phys. Chem. A*, 2017, **121**, 3392–3400.
84 A. J. Lopes Jesus, C. M. Nunes, R. Fausto and I. Reva, *Chem. Commun.*, 2018, **54**, 4778–4781.
85 L. Lapinski, I. Reva, H. Rostkowska, A. J. Lopes Jesus, S. M. Vieira Pinto, R. Fausto and M. J. Nowak, *J. Phys. Chem. A*, 2019, **123**, 3831–3839.
86 A. Halasa, L. Lapinski, H. Rostkowska and M. J. Nowak, *J. Phys. Chem. A*, 2015, **119**, 9262–9271.
87 A. D. Becke, *J. Chem. Phys.*, 1993, **98**, 5648–5652.
88 C.-T. Lee, W.-T. Yang and R. G. Parr, *Phys. Rev. B: Condens. Matter Mater. Phys.*, 1988, **37**, 785–789.
89 S. H. Vosko, L. Wilk and M. Nusair, *Can. J. Phys.*, 1980, **58**, 1200–1211.
90 W. J. Hehre, R. Ditchfield and J. A. Pople, *J. Chem. Phys.*, 1972, **56**, 2257–2261.
91 M. J. Frisch, G. W. Trucks, H. B. Schlegel, G. E. Scuseria, M. A. Robb, J. R. Cheeseman, G. Scalmani, V. Barone, B. Mennucci, G. A. Petersson, H. Nakatsuji, M. Caricato, X. Li, H. P. Hratchian, A. F. Izmaylov, J. Bloino, G. Zheng, J. L. Sonnenberg, M. Hada, M. Ehara, K. Toyota, R. Fukuda, J. Hasegawa, M. Ishida, T. Nakajima, Y. Honda, O. Kitao, H. Nakai, T. Vreven, J. A. Montgomery, Jr., J. E. Peralta, F. Ogliaro, M. Bearpark, J. J. Heyd, E. Brothers, K. N. Kudin, V. N. Staroverov, T. Keith, R. Kobayashi, J. Normand, K. Raghavachari, A. Rendell, J. C. Burant, S. S. Iyengar, J. Tomasi, M. Cossi, N. Rega, J. M. Millam, M. Klene, J. E. Knox, J. B. Cross, V. Bakken, C. Adamo, J. Jaramillo, R. Gomperts, R. E. Stratmann, O. Yazyev, A. J. Austin, R. Cammi, C. Pomelli, J. W. Ochterski, R. L. Martin, K. Morokuma, V. G. Zakrzewski, G. A. Voth, P. Salvador, J. J. Dannenberg, S. Dapprich, A. D. Daniels, O. Farkas, J. B. Foresman, J. V. Ortiz, J. Cioslowski and D. J. Fox, *Gaussian 09, Revision D.01*, Gaussian, Inc., Wallingford CT, 2013.
92 V. Barone, *J. Chem. Phys.*, 2005, **122**, 014108.
93 J. Bloino and V. Barone, *J. Chem. Phys.*, 2012, **136**, 124108.
94 V. Barone, M. Biczysko and J. Bloino, *Phys. Chem. Chem. Phys.*, 2014, **16**, 1759–1787.
95 V. Barone, J. Bloino, C. A. Guido and F. Lipparini, *Chem. Phys. Lett.*, 2010, **496**, 157–161.
96 K. K. Irikura, *SYNSPEC*, National Institute of Standards and Technology, Gaithersburg MD, 1995.
97 S. Grimme, *J. Chem. Phys.*, 2006, **124**, 034108.
98 C.-Y. Peng, P. Y. Ayala, H. B. Schlegel and M. J. Frisch, *J. Comput. Chem.*, 1996, **17**, 49–56.
99 X. Chen, Y.-Y. Zhao, H.-B. Zhang, J.-D. Xue and X.-M. Zheng, *J. Phys. Chem. A*, 2015, **119**, 832–842.
100 B. I. Niefer, H. G. Kjaergaard and B. R. Henry, *J. Chem. Phys.*, 1993, **99**, 5682–5700.
101 B. J. Miller, L. Du, T. J. Steel, A. J. Paul, A. H. Södergren, J. R. Lane, B. R. Henry and H. G. Kjaergaard, *J. Phys. Chem. A*, 2012, **116**, 290–296.
102 S. D. Schrøder, A. S. Hansen, J. H. Wallberg, A. R. Nielsen, L. Du and H. G. Kjaergaard, *Spectrochim. Acta, Part A*, 2017, **173**, 201–206.